Detection of ice wedges in Yedoma along the Dalton Highway, Alaska, USA, using capacitive-coupled electrical resistivity tomography

Richard Fortier[1], William Schnabel[2], Kevin Bjella[3], Mikhail Kanevskiy[2] & Yuri Shur[2]

[1]*Centre d'études nordiques (CEN), Université Laval, Québec City, Québec, Canada*

[2]*University of Alaska Fairbanks (UAF), Fairbanks, Alaska, United States*

[3]*U.S. Army Engineer Research and Development Center (ERDC), Fort Wainwright, Alaska, United States*

ABSTRACT

In the 2000s, the Alaska Department of Transportation investigated the possibility of realigning about 5 km of the Dalton Highway in Alaska, USA, between the Mile Posts 8 and 12, to meet current design standards and provide safer alignments and grades than the current ones. The project area is in the continuous permafrost zone where ice-rich syngenetic permafrost with large ice wedges, known as Yedoma, formed during the late Pleistocene. To achieve a geotechnical investigation for assessing the permafrost conditions along the proposed realignment, a total of 136 boreholes were drilled.

The ground truth coming from these boreholes offers a unique opportunity to assess the capabilities of engineering geophysical investigation in delineating potentially problematic ice-rich permafrost. Therefore, in addition to this geotechnical investigation, ground penetrating radar (GPR) profiling, direct-current and capacitive-coupled electrical resistivity tomographies (DC-ERT and CC-ERT, respectively) were carried out along the proposed realignment. The permafrost table and top of ice-rich syngenetic permafrost were identified in the GPR profile. Both the higher sensitivity and spatial sampling of CC-ERT than DC-ERT allowed the individual detection of resistive ice wedges embedded in more conductive frozen silts in the model of electrical resistivity from the CC-ERT inversion. This is made possible by the high electrical resistivity contrast between ice wedges and frozen silts near 0 °C. In the DC-ERT model, only large zones of resistive ice-rich permafrost were delineated without individually detecting the ice wedges. This case study shows the capabilities of CC-ERT to delineate ice wedges in a warm permafrost environment. Geophysical investigations prior to geotechnical investigations can help in designing cost-effective drilling campaigns with fewer expensive boreholes for ground truth along planned linear infrastructures in permafrost environments.

1 INTRODUCTION

Very long linear infrastructures such as roads and airfields in permafrost environments are vulnerable to permafrost degradation due to not only their impacts on permafrost dynamics but also climate warming. To reduce their vulnerability to permafrost degradation and mitigate the impacts of permafrost degradation on their life span, performance, and maintenance cost, geotechnical investigations including drilling, permafrost sampling, and laboratory testing are carried out along their extent before construction for location planning and design purpose. However, blind geotechnical investigations without gathering a priori information from digital elevation models, aerial photographs, mapping of surficial geology and permafrost conditions, and geophysical investigation are doomed to fail in identifying the zones most vulnerable to permafrost degradation. Moreover, geotechnical investigations with high density and systematic drilling and sampling are very expensive. A way to optimize the investment in a geotechnical investigation and lower cost is to perform an engineering geophysical investigation to assess permafrost conditions and locate ice-rich permafrost zones vulnerable to degradation as targets for geotechnical investigation. But, currently, this approach of performing engineering geophysical investigations prior to geotechnical investigations along planned linear infrastructures in permafrost environments is not the norm in cold regions engineering practice, likely because there is no well-documented case study as a proof of concept showing the advantages by doing so.

The Dalton Highway, or Alaska Route 11, is a 666-km long road in Alaska, USA, which links interior Alaska to Deadhorse near the Arctic Ocean (Figure 1). This highway was built in 1974 as a supply road to support the Trans-Alaska Pipeline System. In the 2000s, the Alaska Department of Transportation (AKDOT) investigated a possible realignment of the Dalton Highway between the Mile Posts (MP) 8 and 12 near Livengood, about 130 km northwest of Fairbanks (Figures 1 and 2), to meet current design standards and provide safer alignments and grades than the current ones. However, this area is in the continuous permafrost zone (Figure 1). The proposed realignment crosses extremely complex permafrost conditions including ice-rich permafrost with large ice wedges (Figure 3), known as Yedoma, which formed syngenetically by simultaneous accumulation of silt and upward permafrost aggradation during the late Pleistocene (Kanevskiy et al. 2012). Evidence of ice-wedge degradation that results in differential thaw subsidence is visible at many places along the Dalton Highway (Figure 4).

https://doi.org/10.52381/ICOP2024.163.1

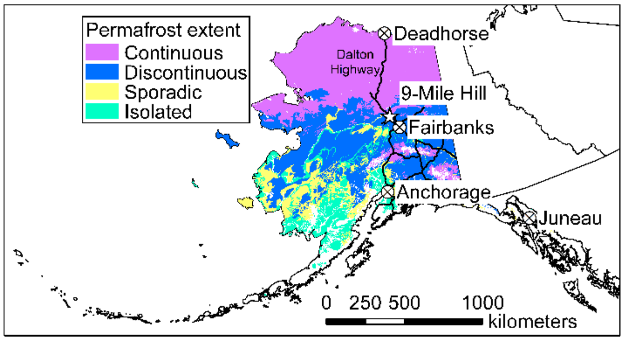

Figure 1. Permafrost map of Alaska, USA (modified from Jorgenson et al., 2008). The star identifies the location of the study site at 9-Mile Hill along the Dalton Highway about 130 km northwest of Fairbanks.

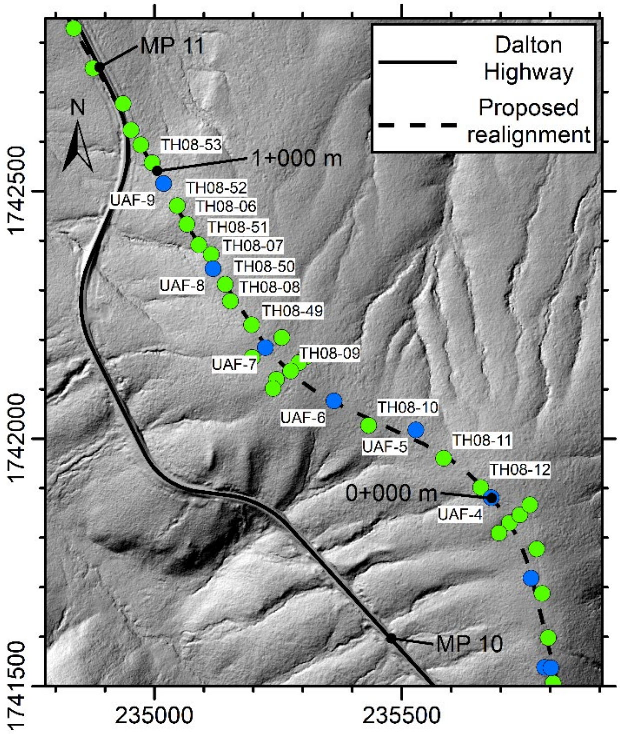

Figure 2. Hillshade map of 9-Mile Hill, Alaska, USA (modified from Hubbard et al. 2011). Location of boreholes drilled for AKDOT (green circles, TH08-XX) and AUTC (blue circles, UAF-X) along the proposed realignment of the Dalton Highway. The Meter Posts 0+000 m and 1+000 m of the geophysical survey line are identified. Projected coordinate system: NAD83 (CORS96) Alaska Albers.

In collaboration with the Alaska University Transportation Center (AUTC) of the University of Alaska Fairbanks (UAF), AKDOT carried out several geotechnical investigations to assess the permafrost conditions along the proposed realignment including 136 boreholes in total (Kanevskiy et al. 2012; Rowland, J. 2010; Schlichting and Darrow 2006; Shur et al. 2010). In Kanevskiy et al. (2012), the main results of these geotechnical investigations are provided such as soils characteristics, local stratigraphy, ice content, and a cryostratigraphic cross-section. The ground truth coming from these geotechnical investigations offers a unique opportunity to assess the capabilities of an engineering geophysical investigation in delineating potentially problematic ice-rich permafrost. The AUTC in collaboration with the Center for Northern Studies (Centre d'études nordiques – CEN) at Université Laval, Québec, Canada, and the U.S. Army Engineer Research and Development Center (ERDC) performed in May 2010 a geophysical investigation including ground penetrating radar (GPR) profiling, direct-current electrical resistivity tomography (DC-ERT), and capacitive-coupled electrical resistivity tomography (CC-ERT) along the proposed realignment of the Dalton Highway (Schnabel et al. 2014). GPR profiling and ERT used along the same survey line are complementary geophysical methods (De Pascale et al. 2008; Fortier and Savard 2010) since ERT is effective to assess the permafrost conditions such as ice-rich zones vs ice-poor or unfrozen zones and GPR can identify the subsurface stratigraphic contacts. The results of this engineering geophysical investigation relative to the borehole logs are presented herein as a proof of concept to show the advantages of performing geophysical surveys prior to geotechnical investigations of permafrost environments. Problematic zones of ice-rich permafrost can be effectively delineated with geophysical investigations, demonstrating that this approach can successfully identify targets for drilling to optimize a cost-effective drilling campaign with fewer boreholes for ground truth.

Figure 3. Ice wedge exposed in a road cut along the Dalton Highway, Alaska, USA. The baseball cap on the right provides the scale. All copyrights reserved to AKDOT.

Figure 4. Localized thaw subsidence zones along the Dalton Highway, Alaska, USA, due to the degradation of ice wedges.

2 METHODOLOGY

A Sensors & Software pulseEKKO Pro with antennas of 100 MHz was used along the realignment of the Dalton Highway on May 20th 2010 to perform two types of surveys: 1) fixed-offset reflection profiling to map the subsurface stratigraphic contacts and 2) common mid-point (CMP) sounding to assess the velocity of the radar signal in the ground. The GPR depth profile corrected for topography is given in Figure 5A. The two CMP soundings 1 and 2 carried out near the boreholes UAF-9 at 0+960 m and UAF-7 at 0+556 m, respectively, along with their analysis are given in Figure 6. The analysis of a GPR-CMP sounding involves stacking the radar traces corrected in time for several velocities to produce a travel time-velocity graph. When the time-corrected traces are stacked at an incorrect velocity, they tend to interfere destructively and to produce low amplitudes of energy on the graph. When they are stacked at a correct velocity, they add together constructively and produce high amplitudes of energy. The highest amplitudes of energy on the travel-time-velocity graph identify the radar-signal velocity.

Measurements of apparent electrical resistivity to achieve the DC-ERT were performed along the survey line from May 7 to 9th 2010 using an Earth Resistivity/IP Meter SUPER STING R1 IP from Advanced Geosciences Inc. This system is made of 4 cables of 21 connectors 2 m apart from each other for a total of 84 metal electrodes, which are driven in the ground for galvanic contact. A Wenner array was used to perform the DC-ERT with a maximum theoretical depth of investigation of about 25 m. The electrodes selection for direct injection of electrical current into the ground and measurement of induced electrical potential was made automatically by the resistivity meter according to an array program previously downloaded in its memory. Once measurements of apparent electrical resistivity were completed after scanning these 84 electrodes, one cable of 21 connectors at the beginning of the survey line was then moved at the end to perform a “roll along” and increase the DC-ERT length. In total, 11 “roll alongs” were performed for an overall DC-ERT length of 628 m and, in total, 5490 measurements of apparent electrical resistivity. The beginning and end of the DC-ERT are at 0+380 m and 1+008 m near the boreholes UAF-6 and TH08-53, respectively (Figure 2).

The apparent electrical resistivities along the survey line were also measured on May 10th 2010 using an OhmMapper TR5 system from Geometrics Ltd. to perform the CC-ERT. This system is made of one transmitter and five receivers as a dipole-dipole configuration. The transmitter and receivers are coaxial cables called line antennas lying on the ground to couple an AC signal at a frequency of about 16.5 kHz into the ground and measure the induced AC signal, respectively. The conductor in the coaxial cable acts as one plate of a capacitor and the ground acts as the other plate while the insulating sheath of the coaxial cable is the capacitor’s insulator. The AC current in the transmitter cable can pass into the ground similarly to an AC signal through a capacitor. The capacitance of the receiver cable is similarly charged, allowing the measurement of an induced AC voltage in the receiver proportional to the electrical resistivity of the ground. This provides an AC equivalent of a standard DC resistivity measurement without the galvanic contacts needed for the standard method (for more details on the theory behind the capacitively-coupled resistivity method, see Timofeev et al. 1994, and Kuras et al. 2006). Since this system does not depend on galvanic contact with electrodes driven in the ground, it can be towed on the ground surface while collecting data for fast engineering geophysical investigation. According to Kuras et al. (2006), the electrical resistivity measurement is emulated through the capacitive coupling when the ground resistivity is high such as permafrost. CC-ERT was successfully used for engineering and environmental geophysical investigations (Douma et al. 1994) of permafrost environments (Calvert 2002; De Pascale et al. 2008; Fortier and Savard 2010) and mountain permafrost (Hauck and Kneisel 2006).

The extremities of the CC-ERT are near the boreholes UAF-4 and TH08-53 (Figure 2) from 0-088 to 1+096 m for 20,973 measurements of apparent electrical resistivity in total. The CC-ERT survey line is longer than the one for the DC-ERT since the production rate in terms of meter per day is much higher for the CC-ERT than the DC-ERT. Only one day was needed to achieve the CC-ERT in comparison to three days for the DC-ERT. Markers at regular 25-m intervals put along the survey line relative to the reference position at borehole UAF-4 (0+000 m) allowed the location of the measurements of apparent electrical resistivity of the CC-ERT. Four runs with the transmitter and five receivers, different dipole lengths and spacings between the dipoles were performed along the survey line (Table 1). The variation in spacing between the current and potential dipoles changes the depth of investigation of the CC-ERT.

Before inversion, during the filtering of the DC-ERT and CC-ERT datasets, 43 and 270 values of apparent electrical resistivity, respectively, were identified as outliers and removed. The filtered datasets were then inverted using a quasi-Newton method (Loke and Barker 1996) and the software package RES2DINV (Geotomo Software 2010) to produce two models of electrical resistivity corrected for topography (Figure 5B, C, respectively).

The line antennas of CC-ERT do not exactly reproduce the dipole-dipole array of galvanic contacts with metal electrodes. The dipole length of CC-ERT is always shorter than the one of DC-ERT (Kuras et al. 2006). The difference in dipole length is the order of 80% (Oldenborger and LeBlanc 2013). Therefore, the values of apparent electrical resistivity measured with CC-ERT are lower than the ones of DC-ERT. No attempt was made to correct the dipole lengths of CC-ERT and ultimately the values of apparent electrical resistivity as proposed by Oldenborger and LeBlanc (2013) before doing the inversion of CC-ERT.

An interpretative cross-section including the borehole logs from the previous drilling campaigns (Kanevskiy et al. 2012; Rowland, J. 2010; Schlichting and Darrow 2006; Shur et al. 2010) modified from Kanevskiy et al. (2012) and the results from the geophysical investigation presented herein is given in Figure 5E.

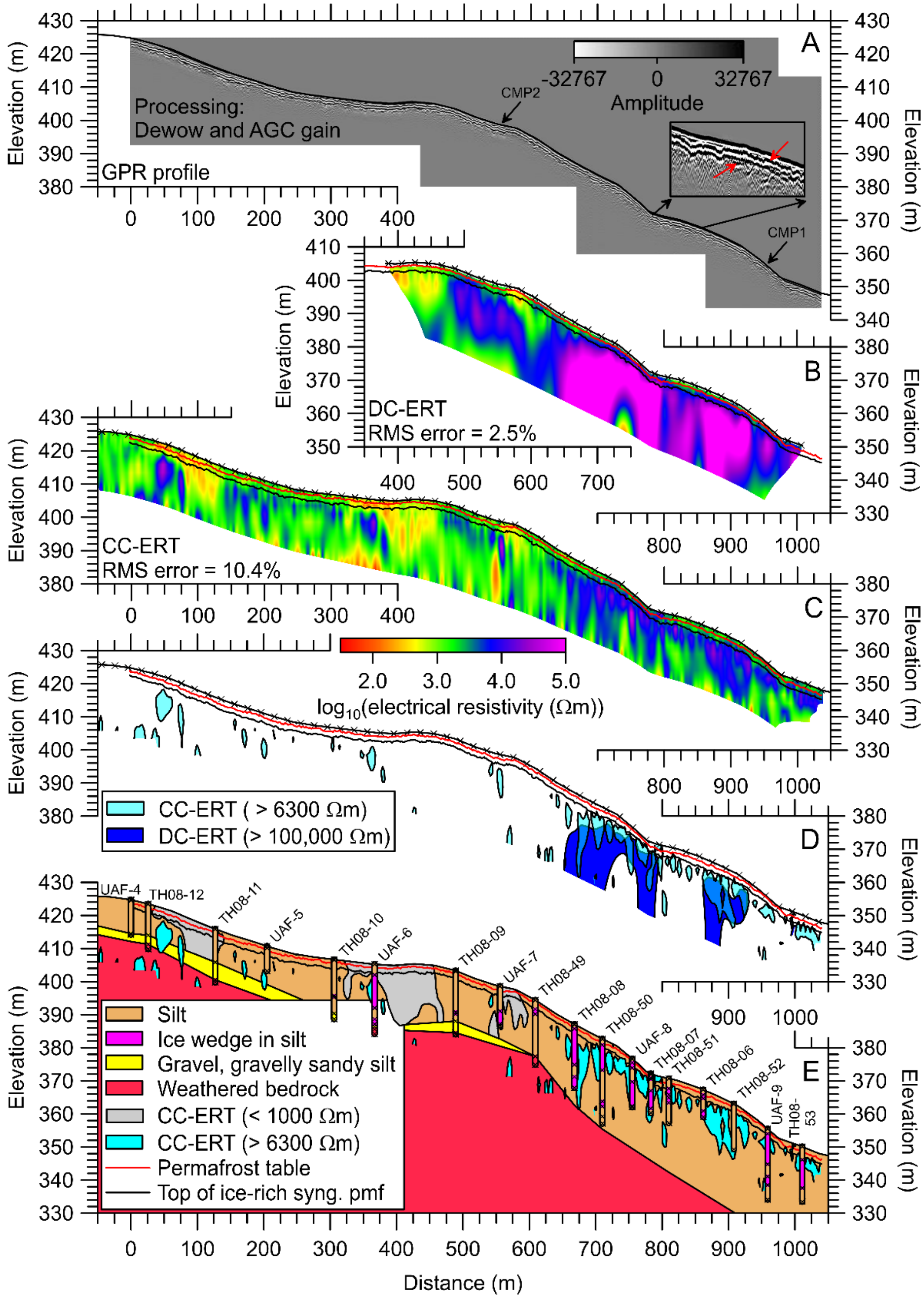

Figure 5. GPR depth profile (A) along the realignment of the Dalton Highway at 9-Mile Hill near Livengood, Alaska, USA (see Figures 1 and 2 for location). Models of electrical resistivity from the inversion of DC-ERT (B) and CC-ERT (C) carried out along the same survey line. (D) Zones of electrical resistivity more than 100,000 Ωm from DC-ERT and 6300 Ωm from CC-ERT. (E) Interpretative cross-section from boreholes (modified from Kanevskiy et al. 2012) along with the results of geophysical investigation. The permafrost table and top of ice-rich syngenetic permafrost as delineated in the GPR profile but not shown are highlighted by red and black full lines, respectively, in the models of electrical resistivity and the interpretative cross-section. Note the vertical exaggeration of 5×.

A thermistor cable driven in the borehole TH08-053 (see Figures 2 and 5 for location) allowed the measurements of ground temperature profiles on August 11th 2008 and May 5th 2010 (Figure 7).

3 RESULTS

From the analysis of the GPR-CMP soundings (Figure 6), the velocity of the radar signal varies between 0.07 (CMP2, Figure 6D) and 0.11 m/ns (CMP1, Figure 6B). A value of 0.1 m/ns was used to transform the GPR travel time profile into a GPR depth profile (Figure 5A).

The scale used in Figure 5 does not allow the identification of reflectors in the GPR profile without zooming in (Figure 5A). Therefore, an inset is provided in Figure 5A to enlarge a small section of the GPR profile and ease the analysis of the GPR profile for that section. Two reflectors as coherent radar signal phases are identified by red arrows in this inset. They are trackable all along the GPR profile, but they are not identified in Figure 5A to avoid any concealing. However, they are highlighted by red and black full lines, respectively, in Figure 5B, C, D, E for comparison purpose.

In the temperature profiles (Figure 7) measured on May 5th 2010, 15 days before performing the GPR surveys, and August 11th 2008, almost at the end of the thawing period, there are unfortunately not enough thermistors to accurately assess the depths of thawing front. A linear interpolation between the ground temperature measurements at depths of 0.8 and 3.8 m as shown by the dashed lines in Figure 7 is not adequate to do so. However, based on the borehole logs, the local stratigraphy is (Kanevskiy et al. 2012): 1) active layer (0–0.7 m), 2) ice-rich silt (0.7–1.5 m), 3) ice-poor thawed and refrozen silt (1.5–3.0 m) and 4) ice-rich syngenetic permafrost (3.0–10.0 m). The two reflectors in the GPR profile are likely due to the stratigraphic contacts between the layers 1 and 2 (permafrost table) and the layers 3 and 4 (top of ice-rich syngenetic permafrost) at respective depths of 0.7 and 3 m. The red and black full lines of these two reflectors are also plotted in the models of electrical resistivity (Figure 5B, C, D) and in the interpretative cross-section for increasing the details (Figure 5E). No other reflector in permafrost was identified at depth in the GPR profile. The depth of investigation of the GPR surveys along the survey line is shallow and limited down to 3 to 4 m deep.

As previously stated, since the CC line antennas are not an equivalent to DC dipoles, the values of electrical resistivity in the CC-ERT model (Figure 5B) are much lower that the ones in the DC-ERT model (Figure 5C). Notwithstanding these differences in electrical resistivity values, the electrical resistivity patterns in both models present striking similitudes and differences while the same permafrost environment was investigated with the two ERT methods. The downhill section of both models of electrical resistivity is more resistive than the uphill section (Figure 5B, C). The change in electrical resistivity behaviour between these two sections is located at about 0+630 m. Since the electrical resistivity is directly proportional to the ice content, one can expect that the ice content of the downhill section is higher than the one of the uphill section. From the analysis of the drilling campaigns (Kanevskiy et al. 2012; Rowland, J. 2010; Schlichting and Darrow 2006; Shur et al. 2010), the downhill and uphill

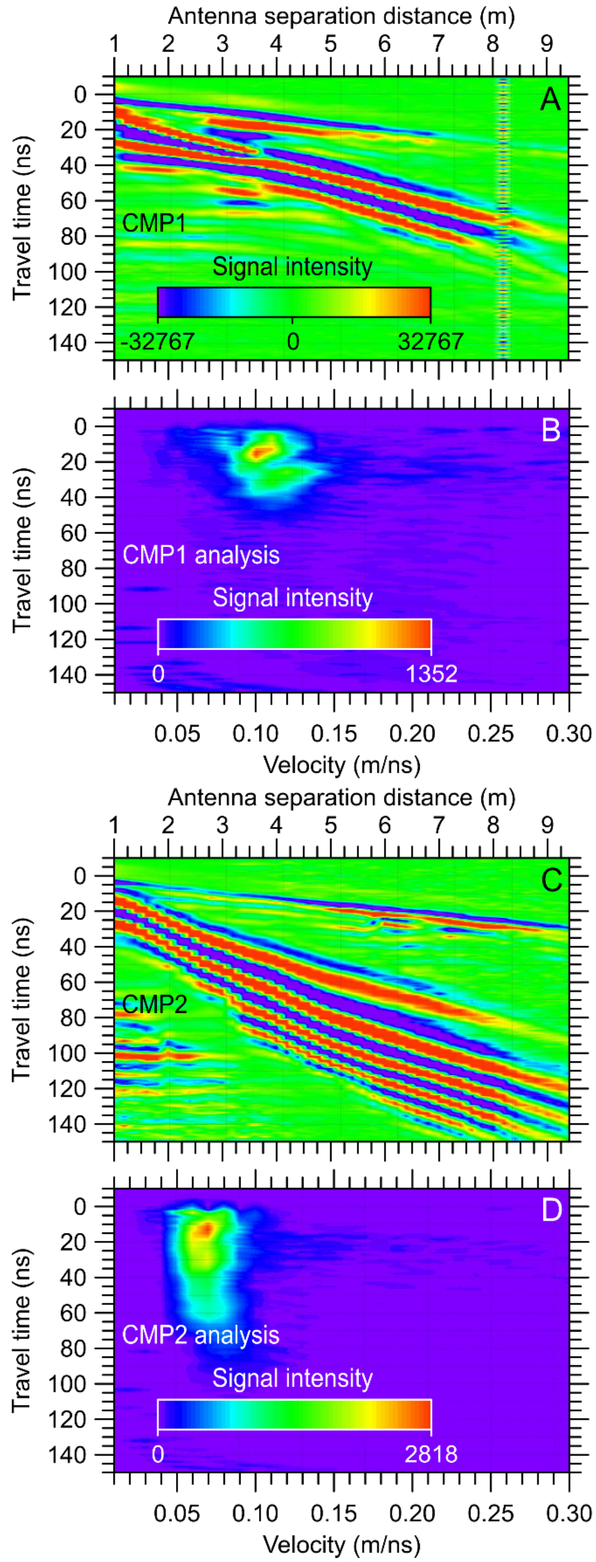

Figure 6. GPR-CMP soundings 1 (A) and 2 (C) carried out near the boreholes UAF-9 at 0+960 m and UAF-7 at 0+556 m, respectively, along the realignment of the Dalton Highway (see Figures 2 and 5 for location). Analysis of GPR-CMP soundings 1 (B) and 2 (D).

Table 1. Parameters used for the CC-ERT.

Run	Electrode cable length, dipole length, and distance between the transmitter dipole and the first receiver dipole (m)	Spacing between the transmitter dipole and the five receiver dipoles (m) (receiver number)	n factor between the dipoles	Theoretical depth of investigation (m) (Loke, 2000)
#1	2.5, 5, and 5	5 (#1)	1	2.1
		7.5 (#2)	1.5	2.8
		10 (#3)	2	3.5
		12.5 (#4)	2.5	4.2
		15 (#5)	3	4.9
#2	5, 10, and 5	5 (#1)	0.5	3.5
		10 (#2)	1	4.9
		15 (#3)	1.5	6.3
		20 (#4)	2	7.7
		25 (#5)	2.5	9.1
#3	5, 10, and 25	25 (#1)	2.5	9.0
		30 (#2)	3	11.0
		35 (#3)	3.5	13.0
		40 (#4)	4	15.0
		45 (#5)	4.5	17.0
#4	5, 10, and 50	50 (#1)	5	14.0
		55 (#2)	5.5	16.0
		60 (#3)	6	18.0
		65 (#4)	6.5	20.0
		70 (#5)	7	22.0

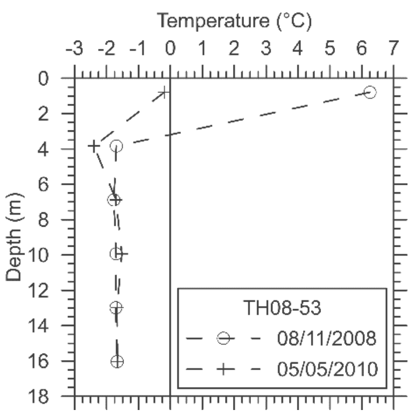

Figure 7. Ground temperature profiles measured along a thermistor cable in the borehole TH08-053 on August 11th 2008 and May 5th 2010 (see Figures 2 and 5 for location).

sections were identified as ice-rich and ice-poor permafrost sections, respectively, in the cross-section developed by Kanevskiy et al. (2012) where the downhill section has a high occurrence of ice wedges (Figure 5E). There is also a superficial layer of low electrical resistivity of about 3 m thick which is due to the units 1, 2, and 3 previously described. The high electrical resistivity contrast in both models at the depth of about 3 m is due to the stratigraphic contact between the units 3 and 4 and corresponds roughly to the second reflector in the GPR profile (see the black full line in both models of electrical resistivity in Figure 5B, C). And, finally, the CC-ERT model looks noisier than the DC-ERT one which is consistent with other studies (Hauck and Kneisel 2006).

4 DISCUSSION

The dipole-dipole array used in the CC-ERT is more sensitive to lateral variations in electrical resistivity than the Wenner array used in the DC-ERT (Dahlin and Zhou 2004). Such lateral variations in electrical resistivity are expected for ice wedges embedded in frozen silts in Yedoma. Moreover, in this study, the spatial sampling of CC-ERT and DC-ERT models is 1748 measurements per 100 m ((20,973 data points – 270 outliers)/survey length of 1184 m) and 867 measurements per 100 m ((5490 data points – 43 outliers)/survey length of 628 m), respectively, for a similar depth of investigation of about 20 m. Both of these higher sensitivity and spatial samplings of CC-ERT than DC-ERT allow the individual detection of resistive ice wedges embedded in more conductive frozen silts in the downhill section of the model of electrical resistivity from the inversion of CC-ERT dataset (Figure 5C). In the DC-ERT, only the bulk electrical resistivity of ice-rich permafrost is visible in the downhill section without individually detecting the ice wedges (Figure 5B).

The delineation of ice-rich permafrost and ice wedges in the downhill section of the DC-ERT and CC-ERT models (Figure 5B, C), respectively, can be done by identifying electrical resistivity limits between ice-poor and ice-rich permafrost and between frozen silt and ice wedges (Figure 5D). To achieve this delineation, electrical resistivity limits of 100,000 Ωm for ice-rich permafrost in the DC-ERT model and 6300 Ωm for ice wedges in the CC-ERT model were empirically assessed. Using these limits, two zones of ice-rich permafrost are delineated, and several ice wedges are individually identified in the downhill section in Figure 5D. As previously stated, the values of electrical resistivity in the CC-ERT model are much lower than the ones in the DC-ERT model. This explains the difference in the two electrical resistivity limits. Instead of using empirical electrical resistivity thresholds, the calculation of electrical resistivity gradients in both models of electrical resistivity would have been another quantitative interpretation criterion not used herein to delineate permafrost conditions based on the identification of the highest gradients (Banville et al. 2016).

The electrical resistivity zonation in the CC-ERT model to delineate ice wedges from frozen silt (Figure 5D) is made possible through the thermal conditions of permafrost at 9-Mile Hill. The permafrost temperature is close to -2 °C (Figure 7). On one hand, at that temperature, the unfrozen water content in frozen silt can be as high as 4% (mass of unfrozen water/mass of dry soil × 100) for a total moisture content of about 55% (Tice et al. 1989) and electrical resistivity is lower than 1000 Ωm (Hoekstra and McNeill 1973). On the other hand, the electrical resistivity of pure ice can be as high as 10 MΩm close to -2 °C (Stillman et al. 2010). Although impurities in ice which are typical for ice wedges can significantly lower the electrical resistivity, there is still a strong electrical resistivity contrast between frozen silt and ice wedges at that temperature. At higher latitudes in the continuous permafrost zone with lower permafrost temperature than 9-Mile Hill, this electrical resistivity contrast with more resistive frozen ground can be lower than the one at 9-Mile Hill. In such cold permafrost environment, CC-ERT may not be as efficient to individually detect ice wedges due to weak electrical resistivity contrast (De Pascale et al. 2008).

The limits of ice wedges in the CC-ERT model (Figure 5D) are also plotted in the cross-section (Figure 5E). Moreover, uphill in both DC-ERT and CC-ERT models, there are zones of very low electrical resistivity below 1000 Ωm. This electrical resistivity limit of 1000 Ωm in the CC-ERT model (Figure 5C) is used to delineate ice-poor permafrost zones and even completely thawed silt which are plotted in the cross-section (Figure 5E). The borehole logs including the units of silt, ice wedge in silt, gravel and gravelly sandy silt, and weathered bedrock, are also superimposed to the previously delineated ice wedges and ice-poor permafrost zones in the cross-section (Figure 5E). This overlay allows the visual correlation of drilled ice wedges and zones of electrical resistivity higher than 6300 Ωm in the CC-ERT model. The agreement between the borehole logs and the CC-ERT model is judged good, such as along the UAF-06 borehole log for instance and with some discrepancies such as for the UAF-09 and TH08-53 borehole logs where the ice wedges are deeper than expected from the interpretation of the CC-ERT model.

There are zones of electrical resistivity higher than 6300 Ωm at depth in the CC-ERT model (Figures 5C, 5D, and 5E). These zones are artefacts from the inversion of ERT dataset as they are located at depth in the bedrock where the CC-ERT model is not well constrained. The depth of investigation of both DC-ERT and CC-ERT is too shallow to detect the weathered bedrock, while the unit of gravel and gravelly sandy silt is probably too thin to be detected.

Based solely on the results from the engineering geophysical investigation along the proposed realignment of the Dalton Highway (Figure 5A, B, C, D), one can design and optimize a drilling campaign to assess the permafrost conditions by identifying targets to drill and sample. For instance, instead of drilling eighteen boreholes along the 1100-m long geophysical survey line (Figure 5E), only the five boreholes TH08-12, TH08-11, UAF-6, UAF-8, and UAF-9 would have been enough to confirm the interpretation of the CC-ERT model for the identification of ice-rich and ice-poor permafrost, and ice wedges. Reduced drilling costs more than offset the costs of an engineering geophysical investigation including GPR profiling and CC-ERT. And, finally, the CC-ERT model can be reinterpreted at the light of borehole logs and constrained inversion can be achieved with these logs (Fortier et al. 2008) instead of free inversion without a priori information as for the present study. From the synthesis of the CC-ERT model and borehole logs, an interpretative cross-section of permafrost conditions can be developed (Figure 5E).

5 CONCLUSIONS

A geotechnical investigation including drilling, soil sampling, and soil testing was carried out in the 2000s along a proposed realignment of the Dalton Highway at 9-Mile Hill near Livengood about 130 km northwest of Fairbanks, Alaska, USA, to assess the permafrost conditions for designing safer alignments and grades than the current ones. The ground truth coming from this geotechnical investigation offers a unique opportunity to assess the capabilities of an engineering geophysical investigation to delineate problematic ice-rich permafrost conditions whose results are presented herein.

Ground penetrating radar profiling identified two stratigraphic contacts (permafrost table and top of ice-rich syngenetic permafrost) all along the survey line. Additionally, two methods of electrical resistivity, using metal electrodes driven in the ground (direct-current electrical resistivity tomography – DC-ERT) and line antennas capacitively coupled with the ground (capacitive-coupled electrical resistivity tomography – CC-ERT), were used to assess the spatial distribution of electrical resistivity. Due to its high production and sampling rate and high sensitivity to lateral variations in electrical resistivity, the CC-ERT has proven to be more efficient to achieve longer survey line in shorter time than the DC-ERT and to individually identify ice wedges.

The results of the geophysical investigation presented herein is a proof of concept of the advantages of performing geophysical surveys prior to geotechnical investigations of permafrost environments. The costs of a drilling campaign can be significatively reduced through its design and optimization by identifying targets in the interpretative geophysical cross-section such as different types of soil, thawed and frozen ground, permafrost table, ice-poor and ice-rich permafrost, and ice wedges.

6 ACKNOWLEDGEMENTS

This work was funded by the Alaska University Transportation Center (Project no. 410018: Geophysical Applications for Arctic/Subarctic Transportation Planning). Thanks are due to William Lee and Erin Trochim, students

at the University of Alaska Fairbanks at the time of the geophysical investigation, for their help in the field and initial processing of DC-ERT survey. The first author acknowledges the welcome of Water and Environment Research Center, University of Alaska Fairbanks, during his sabbatical leave in 2009-2010 when he participated in the geophysical investigation presented herein. Thanks are due to two anonymous reviewers for improving the paper. This paper was written without using artificial intelligence.

7 References

Banville, D., Fortier, R. and Dupuis, C. 2016. 'Objective interpretation of induced polarization tomography using a quantitative approach for the investigation of periglacial environments', *Journal of Applied Geophysics* 130, pp. 218–233.

Calvert, H.T. 2002. 'Capacitive-coupled resistivity survey of ice-bearing sediments, Mackenzie Delta', in *72nd Annual Meeting, Society of Exploration Geophysicists*. Salt Lake City, Utah, United States.

Dahlin. T. and Zhou, B. 2004. 'A numerical comparison of 2D resistivity imaging with 10 electrode arrays', *Geophysical Prospecting* 52(5), pp. 379–398.

De Pascale, G.P., Pollard, W.H. and Williams, K.K. 2008. 'Geophysical mapping of ground ice using a combination of capacitive coupled resistivity and ground-penetrating radar, Northwest Territories, Canada', *Journal of Geophysical Research* 113, F02S90. doi:10.1029/2006JF000585.

Douma, M., Timofeev, V.M., Rogozinski, A.W. and Hunter, J.A. 1994. 'A capacitive-coupled ground resistivity system for engineering and environmental applications; results of two Canadian field tests', in *64th Annual International Meeting, Society of Exploration Geophysicists*. Los Angeles, California, United States: pp. 559–561.

Fortier, R., LeBlanc, A.-M., Buteau, S., Allard, M. and Calmels, F. 2008. 'Internal structure and conditions of permafrost mounds at Umiujaq in Nunavik, Canada, inferred from field investigation and electrical resistivity tomography', *Canadian Journal of Earth Sciences* 45, pp. 367–387.

Fortier, R. and Savard, C. 2010. 'Engineering geophysical investigation of permafrost conditions underneath airfield embankments in Northern Quebec (Canada)', in *6th Canadian Conference on Permafrost (GEOCalgary 2010)*. Calgary, Alberta, Canada: pp. 1307–1314.

Geotomo Software 2010. *RES2DINV: Rapid 2-D Resistivity & IP inversion using the least-squares method.* 151 p.

Hauck, C. and Kneisel, C. 2006. 'Application of capacitively-coupled and DC electrical resistivity imaging for mountain permafrost studies', *Permafrost and Periglacial Processes* 17, pp. 169–177.

Hoekstra, P. and McNeill, D. 1973. 'Electromagnetic probing of permafrost', in *Second International Conference on Permafrost*. Yakutsk, Russia: North American Contribution Volume, pp. 517–526.

Hubbard, T.D., Braun, M.L., Westbrook, R.E. and Gallagher, P.E. 2011. *High-resolution lidar data for infrastructure corridors, Livengood Quadrangle, Alaska* Available at: https://doi.org/10.14509/23023.

Jorgenson, T., Yoshikawa, K., Kanevskiy, M., Shur, Y., Romanovsky, V., Marchenko, S., Grosse, G., Brown, J. and Jones, B. 2008. 'Permafrost characteristics of Alaska', in *Ninth International Conference on Permafrost*. Fairbanks, Alaska, United States: pp. 121–124.

Kanevskiy, M., Shur, Y., Connor, B., Dillon, M., Stephani, E. and O'Donnell, J. 2012. 'Study of Ice-Rich Syngenetic Permafrost for Road Design (Interior Alaska)', in *Tenth International Conference on Permafrost*. Salekhard, Russia: Volume 1, International contributions, pp. 191–196.

Kuras, O., Beamish, D., Meldrum, P.I. and Ogilvy, R.D. 2006. 'Fundamentals of the capacitive resistivity technique', *Geophysics* 71, pp. 135–152.

Loke, M.H., 2000. *Electrical imaging surveys for environmental and engineering studies: A practical guide to 2-D and 3-D surveys*.

Loke, M.H. and Barker R. 1996. 'Rapid least-squares inversion of apparent resistivity pseudo-sections using a quasi-Newton method', *Geophysical Prospecting* 44, pp. 131–152.

Oldenborger, G.A. and LeBlanc, A.-M. 2013. 'Capacitive resistivity inversion using effective dipole lengths for line antennas', *Journal of Applied Geophysics* 98, pp. 229–236.

Rowland, J. 2010. 'Geotechnical report – supplemental, Dalton Highway 9 mile North', *Alaska Department of Transportation and Public Facilities, Northern Region Material Section*, Federal Project No. NHF-06502(3) / State Project No. 64899.

Schlichting, S.J. and Darrow, M.M. 2006. 'Geotechnical report, Dalton Highway 9 mile Hill North', *Alaska Department of Transportation and Public Facilities, Northern Region*, Federal Project No. NH-F-065-2(3) / State Project No. 64899.

Schnabel, W., Fortier, R., Kanevskiy, M., Munk, J., Shur, Y. and Trochim, E. 2014. 'Geophysical applications for arctic/subarctic transportation planning, Final Report', *Alaska University Transportation Center* Project # 410018, INE/AUTC 13.01.

Stillman, D.E., Grimm, R.E. and Dec, S.F. 2010. 'Low-frequency electrical properties of ice-silicate mixtures', *Journal of Physical Chemistry B* 114, pp. 6065–6073.

Shur, Y, Kanevskiy, M, Dillon, M, Stephani, E. and O'Donnell, J. 2010. 'Geotechnical investigations for the Dalton Highway innovation project as a case study of the ice-rich syngenetic permafrost', *Institute of Northern Engineering, University of Alaska Fairbanks* Report # FHWA-AK-RD-10-06, prepared for AK DOT & PF, AUTC assigned project # 207122.

Tice, A.R., Black, P.B. and Berg, R.L. 1989. ‘Unfrozen water contents of undisturbed and remolded Alaskan silt’, *Cold Regions Science and Technology* 17, pp. 103–111.

Timofeev, V.M., Rogozinski, A.W., Hunter, J.A. and Douma, M. 1994. ‘A new ground resistivity method for engineering and environmental geophysics’, in *Proceedings of the Symposium on the Application of Geophysics to Engineering and Environmental Problems*, EEGS, pp. 701–15.